

# Object Detection for Graphical User Interface: Old Fashioned or Deep Learning or a Combination?

Anonymous Author(s)

## ABSTRACT

Detecting Graphical User Interface (GUI) elements in GUI images is a domain-specific object detection task. It supports many software engineering tasks, such as GUI animation and testing, GUI search and code generation. Existing studies for GUI element detection directly borrow the mature methods from computer vision (CV) domain, including old fashioned ones that rely on traditional image processing features (e.g., canny edge, contours), and deep learning models that learn to detect from large-scale GUI data. Unfortunately, these CV methods are not originally designed with the awareness of the unique characteristics of GUIs and GUI elements and the high localization accuracy of the GUI element detection task. We conduct the first large-scale empirical study of seven representative GUI element detection methods on over 50k GUI images to understand the capabilities, limitations and effective designs of these methods. This study not only sheds the light on the technical challenges to be addressed but also informs the design of new GUI element detection methods. We accordingly design a new GUI-specific old-fashioned method for non-text GUI element detection which adopts a novel top-down coarse-to-fine strategy, and incorporate it with the mature deep learning model for GUI text detection. Our evaluation on 25,000 GUI images shows that our method significantly advances the start-of-the-art performance in GUI element detection.

## 1 INTRODUCTION

GUI allows users to interact with software applications through graphical elements such as widgets, images and text. Recognizing GUI elements in a GUI is the foundation of many software engineering tasks, such as GUI automation and testing [4, 30, 43, 45], supporting advanced GUI interactions [1, 12], GUI search [11, 34], and code generation [9, 26, 28]. Recognizing GUI elements can be achieved by instrumentation-based or pixel-based methods. Instrumentation-based methods [3, 23, 29] are intrusive and requires the support of accessibility APIs [6, 19] or runtime infrastructures [18, 25] that expose information about GUI elements within a GUI. In contrast, pixel-based methods directly analyze the image of a GUI, and thus are non-intrusive and generic. Due to the cross-platform characteristics of pixel-based methods, they can be widely used for novel applications such as robotic testing of touch-screen applications [30], linting of GUI visual effects [47] in both Android and IOS.

Pixel-based recognition of GUI elements in a GUI image can be regarded as a domain-specific object detection task. Object detection is a computer-vision technology that detects instances of semantic objects of a certain class (such as human, building, or car) in digital images and videos. It involves two sub-tasks: *region detection or proposal* - locate the bounding box (bbox for short) (i.e., the smallest rectangle region) that contains an object, and *region classification* - determine the class of the object in the bounding box. Existing object-detection techniques adopt a bottom-up strategy: starts with primitive shapes and regions (e.g., edges or contours) and aggregate

them progressively into objects. Old-fashioned techniques [26, 28, 40] relies on image features and aggregation heuristics generated by expert knowledge, while deep learning techniques [13, 33, 35] use neural networks to learn to extract features and their aggregation rules from large image data.

GUI elements can be broadly divided into text elements and non-text elements (see Figure 1 for the examples of Android GUI elements). Both old-fashioned techniques and deep learning models have been applied for GUI element detection [8, 26, 28, 43, 46]. As detailed in Section 2.1, considering the image characteristics of GUIs and GUI elements, the high accuracy requirement of GUI-element region detection, and the design rationale of existing object detection methods, we raise a set of research questions regarding the effectiveness features and models originally designed for generic object detection on GUI elements, the region detection accuracy of statistical machine learning models, the impact of model architectures, hyperparameter settings and training data, and the appropriate ways of detecting text and non-text elements.

These research questions have not been systematically studied. First, existing studies [26, 28, 43] evaluate the accuracy of GUI element detection by only a very small number (dozens to hundreds) of GUIs. The only large-scale evaluation is GUI component design gallery [8], but it tests only the default anchor-box setting of Faster RCNN [35] (a two-stage model). Second, none of existing studies (including [8]) have investigated the impact of training data size and anchor-box setting on the performance of deep learning object detection models. Furthermore, the latest development of anchor-free object detection has never been attempted. Third, no studies have compared the performance of different methods, for example old fashioned versus deep learning, or different styles of deep learning (e.g., two stage versus one stage, anchor box or free). Fourth, GUI text is simply treated by Optical Character Recognition (OCR) techniques, despite the significant difference between GUI text and document text that OCR is designed for.

To answer the raised research questions, we conduct the first large-scale, comprehensive empirical study of GUI element detection methods, involving a dataset of 50,524 GUI screenshots extracted from 8,018 Android mobile applications (see Section 3.2.1), and two representative old-fashioned methods (REMAUI [28] and Xianyu [46]) and three deep learning models (Faster RCNN [35], YOLOv3 [33] and CenterNet [13]) that cover all major method styles (see Section 3.2.2). Old-fashioned detection methods perform poorly (REMAUI  $F_1=0.201$  and Xianyu  $F_1=0.117$  at  $IoU>0.9$ ) for non-text GUI element detection. IoU is the intersection area over union area of the detected bounding box and the ground-truth box. Deep learning methods perform much better than old-fashioned methods, and the two-stage anchor-box based Faster RCNN performs the best ( $F_1=0.438$  at  $IoU>0.9$ ), and demands less training data. However, even Faster RCNN cannot achieve a good balance of the coverage of the GUI elements and the accuracy of the detected

bounding boxes. It is surprising that anchor-box based models are robust to the anchor-box settings, and merging the detection results by different anchor-box settings can improve the final performance. Our study shows that detecting text and non-text GUI elements by a single model performs much worse than by a dedicated text and non-text model respectively. GUI text should be treated as scene text rather than document text, and the state-of-the-art deep learning scene text model EAST [49] (pretrained without fine tuning) can accurately detect GUI text.

Inspired by these findings, we design a novel approach for GUI element detection. For non-text GUI element detection, we adopt the simple two-stage architecture: perform region detection and region classification in a pipeline. For non-text region detection, we prefer the simplicity and the bounding-box accuracy of old-fashioned methods. By taking into account the unique boundary, shape, texture and layout characteristics of GUI elements, we design a novel old-fashioned method with a top-down coarse-to-fine detection strategy, rather than the current bottom-up edge/contour aggregation strategy in existing methods [28, 46]. For non-text region classification and GUI text detection, we adopt the mature, easy-to-deploy ResNet50 image classifier [20] and the EAST scene text detector [49], respectively. By a synergy of our novel old-fashioned methods and existing mature deep learning models, our new method achieves 0.573 in F1 for all GUI elements, 0.523 in F1 for non-text GUI elements, and 0.516 in F1 for text elements in a large-scale evaluation with 25,000 GUI images, which significantly outperform existing old-fashioned methods, and outperform the best deep learning model by 19.4% increase in F1 for non-text elements and 47.7% increase in F1 for all GUI elements.

This paper makes the following contributions:

- We perform the first systematic analysis of the problem scope and solution space of GUI element detection, and identify the key challenges to be addressed, the limitations of existing solutions, and a set of unanswered research questions.
- We conduct the first large-scale empirical study of seven representative GUI element detection methods, which systematically answers the unanswered questions. We identify the pros and cons of existing methods which informs the design of new methods for GUI element detection.
- We develop a novel approach that effectively incorporates the advantages of different methods and achieves the state-of-the-art performance in GUI element detection.

## 2 PROBLEM SCOPE AND SOLUTION SPACE

In this section, we identify the unique characteristics of GUIs and GUI elements, which have been largely overlooked when designing or choosing GUI element detection methods (Section 2.1). We also summarize representative methods for GUI element detection and point out the challenges that the unique characteristics of GUIs and GUI elements pose to these methods (Section 2.2).

### 2.1 Problem Scope

Figure 1 and Figure 6 shows examples of GUI elements and GUIs in our dataset. We observe two element-level characteristics: large in-class variance and high cross-class similarity, and two GUI-level characteristics: packed scene and close-by elements, and mix of

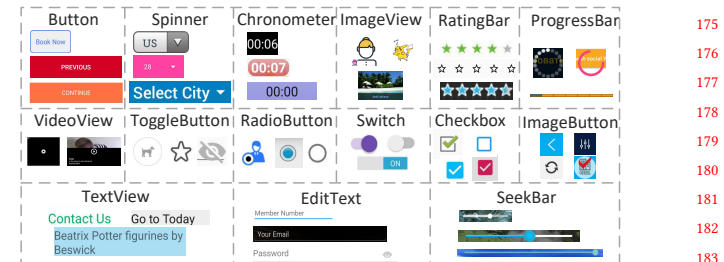


**Figure 1: Characteristics of GUI elements: large in-class variance and high cross-class similarity**

heterogeneous objects. In face of these characteristics, GUI element detection must achieve high accuracy on region detection.

**Large in-class variance:** GUI elements are artificially designed, and their properties (e.g., height, width, aspect ratio and textures) depend on the content to display, the interaction to support and the overall GUI designs. For example, the width of Button or EditText depends on the length of displayed texts. ProgressBar may have different styles (vertical, horizontal or circle). ImageView can display images with any objects or contents. Furthermore, different designers may use different texts, colors, backgrounds and look-and-feel, even for the same GUI functionality. In contrast, physical-world objects, such as human, car or building, share many shape, appearance and physical constraints in common within one class. Large in-class variance of GUI elements pose main challenge of accurate region detection of GUI elements.

**High cross-class similarity:** GUI elements of different classes often have similar size, shape and visual features. For example, Button, Spinner and Chronometer all have rectangle shape with some text in the middle. Both SeekBar and horizontal ProgressBar show a bar with two different portions. The visual differences to distinguish different classes of GUI elements can be subtle. For example, the difference between Button and Spinner lies in a small triangle at the right side of Spinner, while a thin underline distinguishes EditText from TextView. Small widgets are differentiated by small visual cues. Existing object detection tasks usually deal with physical objects with distinct features across classes, for example, horses, trucks, persons and birds in the popular COCO2015 dataset [24]. High cross-class similarity affects not only region classification but also region detection by deep learning models, as these two subtasks are jointly trained.

**Mix of heterogeneous objects:** GUIs display widgets, images and texts. Widgets are artificially rendered objects. As discussed above, they have large in-class variance and high cross-class similarity. ImageView has simple rectangle shape but can display any contents and objects. For the GUI element detection task, we want to detect the ImageViews themselves, but not any objects in the images. However, the use of visual features designed for physical objects (e.g., canny edge [7], contour map [39]) contradicts this goal. In Figure 6, we can observe a key difference between GUI texts and general document texts. That is, GUI texts are often highly cluttered with the background and close to other GUI elements, which pose main challenge of accurate text detection. These heterogeneous properties of GUI elements must be taken into account when designing GUI element detection methods.

**Packed scene and close-by elements:** As seen in Figure 6, GUIs, especially those of mobile applications, are often packed with

**Table 1: Existing solutions for non-text GUI element detection and their limitations**

Style	Method	Region Detection	Region Classification
Old Fashioned	Edge/contour aggregation [26, 28, 46]	<ul style="list-style-type: none"> <li>• Detect primitive edges and/or regions, and merge them into larger regions (windows or objects)</li> <li>• Merge with text regions recognized by OCR</li> <li>• Ineffective for artificial GUI elements (e.g., images)</li> </ul>	Heuristically distinguish image, text, list, container [28, 46]. Can be enhanced by a CNN classification like in [26]
	Template matching [2, 12, 30, 45]	<ul style="list-style-type: none"> <li>• Depend on manual feature engineering (either sample images or abstract prototypes)</li> <li>• Match samples/prototypes to detect object bounding box and class at the same time</li> <li>• Only applicable to simple and standard GUI elements (e.g., button, checkbox)</li> <li>• Hard to apply to GUI elements with large variance of visual features</li> </ul>	
Deep Learning	Anchor-box, two stage [8, 35]	<ul style="list-style-type: none"> <li>• Must define anchor boxes</li> <li>• Pipeline region detection and region classification</li> <li>• Gallery D.C. [8] is the only work that tests the Faster RCNN on large-scale real GUIs, but it uses default settings</li> </ul>	A CNN classifier for region classification, trained jointly with region proposal network
	Anchor-box, one stage [33, 43]	<ul style="list-style-type: none"> <li>• YOLOv2 [32] and YOLOv3 [33] uses k-means to determine anchor boxes (k is user-defined)</li> <li>• Simultaneously region detection and region classification</li> <li>• [43] uses YOLOv2; trains and tests on artificial desktop GUIs; only tests on 250 real GUIs</li> </ul>	
	Anchor free [13]		Never applied

many GUI elements, covering almost all the screen space. In our dataset (see Section 3.2.1), 77% of GUIs contain more than seven GUI elements. Furthermore, GUI elements are often placed close side by side and separated by only small padding in between. In contrast, there are only an average of seven objects placed sparsely in an image in the popular COCO(2015) object detection challenge [24]. GUI images can be regarded as packed scenes. Detecting objects in packed scenes is still a challenging task, because close-by objects interfere the accurate detection of each object’s bounding box.

**High accuracy of region detection** For generic object detection, a typical correct detection is defined loosely, e.g., by an IoU > 0.5 between the detected bounding box and its ground truth (e.g., the PASCAL VOC Challenge standard [15]), since people can recognize an object easily from major part of it. In contrast, GUI element detection has a much stricter requirement on the accuracy of region detection. Inaccurate region detection may not only result in inaccurate region classification, but more importantly it also significantly affects the downstream applications, for example, resulting in incorrect layout of generated GUI code, or clicking on the background in vain during GUI testing. However, the above GUI characteristics make the accurate region detection a challenging task. Note that accurate region classification is also important, but the difficulty level of region classification relies largely on the downstream applications. It can be as simple as predicting if a region is tapable or editable for GUI testing, or if a region is a widget, image or text in order to wireframe a GUI, or which of dozens of GUI framework component(s) can be used to implement the region.

## 2.2 Solution Space

We summarize representative methods for GUI element detection, and raise questions that have not been systematically answered.

**2.2.1 Non-Text Element Detection.** Table 1 summarizes existing methods for non-text GUI element detection. By contrasting these methods and the GUI characteristics in Section 2.1, we raise a series of questions for designing effective GUI element detection methods.

We focus our discussion on region detection, which aims to distinguish GUI element regions from the background. Region classification can be well supported by a CNN-based image classifier [26].

**The effectiveness of physical-world visual features.** Old-fashioned methods for non-text GUI element detection rely on either edge/contour aggregation [26, 28, 46] or template matching [2, 12, 30, 45]. Canny edge [7] and contour map [39] are primitive visual features of physical-world objects, which are designed to capture fine-grained texture details of objects. However, they do not intuitively correspond to the shape and composition of GUI elements. It is error-prone to aggregate these fine-grained regions into GUI elements, especially when GUIs contain images with physical-world objects. Template matching methods improve over edge/contour aggregation by guiding the region detection and aggregation with high-quality sample images or abstract prototypes of GUI elements. But this improvement comes with the high cost of manual feature engineering. As such, it is only applicable to simple and standard GUI widgets (e.g., button and checkbox of desktop applications). It is hard to apply template-matching method to GUI elements of mobile applications which have large variance of visual features. Deep learning models [8, 13, 33, 35, 43] remove the need of manual feature engineering by learning GUI element features and their composition from large numbers of GUIs. *How effective can deep learning models learn GUI element features and their composition in face of the unique characteristics of GUIs and GUI elements?*

**The accuracy of bounding box regression.** Deep learning based object detection learns a statistical regression model to predict the bounding box of an object. This regression model makes the prediction in the feature map of a high layer of the CNN, where one pixel stands for a pixel block in the original image. *Can such statistical regression satisfy the high-accuracy requirement of region detection, in face of large in-class variance of GUI element and packed or close-by GUI elements?*

**The impact of model architectures, hyperparameters and training data.** Faster RCNN [35] and YOLOv2 [33] have been applied to GUI element detection. These two models rely on a set of pre-defined anchor boxes. The number of anchor boxes and their

height, width and aspect ratio are all the model hyperparameters, which are either determined heuristically [35] or by clustering the training images using k-means and then using the metrics of the centroid images [33]. Considering large in-class variance of GUI elements, *how sensitive are these anchor-box based models to the definition of anchor boxes, when they are applied to GUI element detection?* Furthermore, the recently proposed anchor-free model (e.g., CenterNet [13]) removes the need of pre-defined anchor-boxes, but has never been applied to GUI element detection. *Can anchor-free model better deal with large in-class variance of GUI elements?* Last but not least, the performance of deep learning models heavily depends on sufficient training data. *How well these models perform with different amount of training data?*

**2.2.2 Text Element Detection.** Existing methods either do not detect GUI texts or detect GUI texts separately from non-text GUI element detection. They simply use off-the-shelf OCR tools (e.g., Tesseract [37]) for GUI text detection. OCR tools are designed for recognizing texts in document images, but GUI texts are very different from document texts. *Is OCR really appropriate for detecting GUI texts? Considering the cluttered background of GUI texts, would it better to consider GUI text as scene text? Can the deep learning scene text model effectively detect GUI texts?* Finally, considering the heterogeneity of GUI widgets, images and texts, *can a single model effectively detect text and non-text elements?*

### 3 EMPIRICAL STUDY

To answer the above unanswered questions, we conduct the first large-scale empirical study of using both old-fashioned and deep learning methods for GUI element detection. Our study is done on a dataset of 50,524 GUI screenshots from the Rico dataset [11], which were extracted from 8,018 Android mobile applications from 27 application categories. Our study involves a systematic comparison of two old-fashioned methods, including the representative method REMAUI [28] in the literature and the method Xianyu [46] recently developed by the industry, and three popular deep learning methods that cover all major model design styles, including two anchor-box based methods - Faster RCNN [35] (two stage style) and YOLO V3 [33] (one stage style) and one one-stage anchor-free model CenterNet [13]. For GUI text detection, we compare OCR tool Tesseract [37] and scene text detector EAST [49], and compare separate and unified detection of text and non-text GUI elements.

#### 3.1 Research Questions

As region classification can be well supported by a CNN-based image classifier [26], the study focuses on three research questions (RQs) on region detection in GUI element detection task:

- **RQ1 Performance:** How effective can different methods detect the region of non-text GUI elements, in terms of the accuracy of predicted bounding boxes and the coverage of GUI elements?
- **RQ2 Sensitivity:** How sensitive are deep learning techniques to anchor-box settings and amount of training data?
- **RQ3 Text detection:** Does scene text recognition fit better for GUI text detection than OCR technique? Which option, separated versus unified text and non-text detection, is more appropriate?

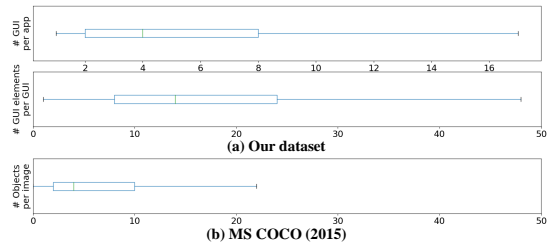


Figure 2: GUI elements distribution in our dataset

### 3.2 Experiment Setup

**3.2.1 Dataset.** We leverage Rico dataset [11] to construct our experimental dataset. In this study, we consider 15 types of commonly used GUI elements in the Android Platform (see examples in Figure 1). We obtain 50,524 GUI screenshots that contain at least one of these 15 types of GUI elements. These GUIs are from 8,018 Android mobile applications of 27 categories. For all methods, the input GUI images is of 608 × 1024 pixels. These GUIs contain 923,404 GUI elements, among which 426,404 are non-text elements and 497,000 are text elements. We remove the standard OS status and navigation bars from all GUI screenshots as they are not part of application GUIs. We obtain the bounding-box and class of the GUI elements from the corresponding GUI metadata. Figure 2 shows the distribution of GUIs per application and the number of GUI elements per image. Compared with the number of objects per image in COCO2015, our GUI images are much more packed. We split these 50,524 GUIs into train/validation/test dataset with a ratio of 8:1:1 (40K:5K:5k). All GUIs of an application will be in only one split to avoid the bias of “seen samples” across training, validation and testing. We perform 5-fold cross-validation in all the experiments.

**3.2.2 Baselines.** The baseline methods used in this study include:

**REMAUI** [28] detects text and non-text elements separately. For text elements, it uses the OCR tool Tesseract [37]. For non-text elements, it detects the edge of GUI elements using Canny edge’s detection [7], then performs edge merging, obtains the contours and gets the bounding box of the GUI elements by merging partial overlapping regions. We use the REMAUI tool [38] provided by its authors in our experiments.

**Xianyu** [46] is a tool developed by the Alibaba to generate code from GUI images. We only use the element detection part of this tool. Xianyu binarizes the image and performs horizontal/vertical slicing recursively to obtain the GUI elements. It uses the edge detection method with laplacian algorithm to detect the edges and get contours in the binarized image. Then, it leverages the flood fill algorithm [42] to identify the connected regions and filters out the noise from the complex background.

**Faster RCNN** [35] is a two-stage anchor-box-based deep learning technique for object detection. It first generates a set of region proposals by a region proposal network (RPN), also called as region of interests (RoIs), which likely contain objects. RPN uses a set of user-defined anchor boxes with different scales and aspect ratios, and computes an objectness score to determine whether the box contains an object or not, and regresses the bounding box for each box. The second stage is a CNN-based image classifier that determines the object class in the RoIs.

465 YOLOv3 [33] is an one-stage anchor-box-based object detection  
 466 technique. Different from the manually-defined anchor box of  
 467 Faster-RCNN, YOLOv3 uses  $k$ -means method to cluster the ground  
 468 truth bounding boxes in the training dataset, and takes the box  
 469 scale and aspect ratio of the  $k$  centroids as the anchor boxes. It also  
 470 extracts image features using CNN, and for each grid of the feature  
 471 map, it then generates a set of bounding boxes. For each box, it  
 472 computes the objectness scores, regresses the box coordinates and  
 473 classifies the object in the bounding box at the same time.

474 CenterNet [13] is an one-stage anchor-free object detection  
 475 technique. Instead of generating bounding box based on the pre-  
 476 defined anchor boxes, it predicts the position of the top-left and  
 477 bottom-right corners and the center of an object, and then assem-  
 478 blies them to get the bounding box of an object. It computes the  
 479 distance between each top-left corner and each bottom-right corner,  
 480 and outputs the bounding box of the matched pair if the distance  
 481 of them is smaller than a threshold and the center point of the  
 482 bounding box has a certerness score higher than a threshold.

483 Tesseract [37] is an OCR tool for document texts. It consists of  
 484 two steps: text line detection and text recognition. Only the text  
 485 line detection is relevant to our study. The Tesseract's text line  
 486 detection is old-fashioned. It first converts the image into binary  
 487 map, and then performs a connected component analysis to find  
 488 the outlines of the elements. These outlines are then grouped into  
 489 blobs, which are further merged together. Finally, it merges text  
 490 lines that overlap at least half horizontally.

491 EAST [49] is a deep learning technique to detect text in natural  
 492 scenes. An input image is first fed into a feature pyramid network.  
 493 EAST then computes six values for each point based on the final  
 494 feature map, namely, an objectness score, top/left/bottom/right  
 495 offsets and a rotation angle. For this baseline, we directly use the  
 496 pre-trained model to detect texts in GUIs without any fine-tuning.

497 3.2.3 *Model Training.* For faster RCNN, YOLOv3 and CenterNet,  
 498 we initialize their parameters using the corresponding pre-trained  
 499 models of COCO object detection dataset and fine-tune all parame-  
 500 ters using our GUI training dataset. We train each model for 160  
 501 iterations with a batch size of 8, and use Adam as the optimizer.  
 502 Faster RCNN uses ResNet-101 [20] as the backbone. YOLOv3 uses  
 503 Darknet-53[33] as the backbone. CenterNet uses Hourglass-52 [44]  
 504 as the backbone. We perform non-maximum suppression (NMS)  
 505 with a IoU threshold of 0.7, and find the best object confidence  
 506 threshold for each model using the validation dataset.

507 3.2.4 *Metrics.* For region detection evaluation, we ignore the class  
 508 prediction results and only evaluate the ability of different methods  
 509 to detect the bounding box of GUI elements. We use precision,  
 510 recall and F1-score to measure the performance of region detection.  
 511 Precision is  $TP/(TP+FP)$  and recall is  $TP/(TP+FN)$ . True positive  
 512 (TP) refers to a detected bounding box which matches a ground  
 513 truth box. False positive (FP) refers to a detected box which does not  
 514 match any ground truth boxes. False negative (FN) refers to a ground  
 515 truth bounding box which is not matched by any detected boxes.  
 516 We compute F1-score as:  $F1 = (2 \times Precision \times Recall) / (Precision + Recall)$ . TP is determined based on the Intersection over Union  
 517 (IoU) of the two boxes. IoU is calculated by dividing the intersection  
 518 area  $I$  of the two boxes  $A$  and  $B$  by the union area of the two boxes,  
 519 i.e.,  $I/(A+B-I)$ . A detected box is considered as a TP if the highest

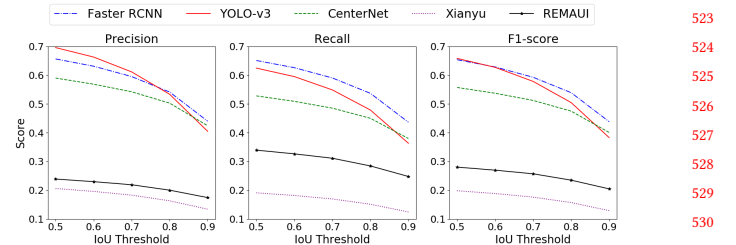


Figure 3: Performance at different IoU thresholds

Table 2: Performance: non-text element detection (IoU&gt;0.9)

Method	#bbox	Precision	Recall	F1
REMAUI	53,903	0.175	0.238	0.201
Xianyu	31,082	0.134	0.104	0.117
Faster-RCNN	39,995	<b>0.440</b>	<b>0.437</b>	<b>0.438</b>
YOLOv3	36,191	0.405	0.363	0.383
CenterNet	36,096	0.424	0.380	0.401

IoU of this box with any ground-truth boxes in the input GUI image is higher than a predefined IoU threshold. Each ground truth box can only be matched at most once and NMS technique is used to determine the optimal matching results. Considering the high accuracy requirement of GUI element detection, we take the IoU threshold 0.9 in most of our experiments.

### 3.3 Results - RQ1 Performance

This section reports the performance of five methods for detecting the regions of non-text GUI elements in a GUI. In this RQ, Faster RCNN uses the customized anchor-box setting and YOLOv3 uses  $k=9$  (see Section 3.4.1). The models are trained using all 40k training data and tested on 5k GUI images in 5-fold cross validation setting.

3.3.1 *Trade off between bounding-box accuracy and GUI-element coverage.* Figure 3 shows the performance of five methods at different IoU thresholds. The F1-score of all deep learning models drop significantly when the IoU threshold increases from 0.5 to 0.9, with the 31%, 45% and 28% decrease for Faster-RCNN, YOLOv3 and CenterNet respectively. The bounding box of a ROI is predicted by statistical regression in the high-layer feature map of the CNN, where one pixel in this abstract feature map corresponds to a pixel block in the original image. That is, a minor change of the predicted coordinates in the abstract feature map will lead to a large change in the exact position in the original image. Therefore, deep learning models either detect more elements with loose bounding boxes or detect less elements with accurate bounding boxes. In contrast, the F1-score of REMAUI and Xianyu does not drop as significantly as that of deep learning models as the IoU threshold increases, but their F1-scores are much lower than those of deep learning models. This suggests that the detected element regions by these old-fashioned methods are mostly noise, but when they do locate real elements, the detected bounding boxes are fairly accurate.

3.3.2 *Performance Comparison.* We observe that if the detected bounding box has  $<0.9$  IoU over the corresponding GUI element, not only does the box miss some portion of this element, but it also includes some portions of adjacent elements due to the packed characteristic of GUI design. Therefore, we use  $\text{IoU} > 0.9$  as an

acceptable accuracy of bounding box prediction. Table 2 shows the overall performance of the five methods at IoU>0.9 threshold for detecting non-text GUI elements.

Xianyu performs the worst, with all metrics below 0.14. We observe that Xianyu works fine for simple GUIs, containing some GUI elements on a clear or gradient background (e.g., Xianyu-(c)/(d) in Figure 6). When the GUI elements are close-by or placed on a complex background image, Xianyu's slicing method and its background de-noising algorithms do not work well. For example, in Xianyu-(a)/(b) in Figure 6, it misses most of GUI elements. Xianyu performs slicing by the horizontal or vertical lines across the whole GUI. Such lines often do not exist in GUIs, especially when they have complex background images (Xianyu-(a)) or the GUI elements are very close-by (Xianyu-(b)). This results in many under-segmentation of GUI images and the misses of many GUI elements. Furthermore, Xianyu sometimes may over-segment the background image (Xianyu-(a)), resulting in many noise non-GUI-element regions.

REMAUI performs better than Xianyu, but it is still much worse than deep learning models. REMAUI suffers from similar problems as Xianyu, including ineffective background de-noising and over-segmentation. It outperforms Xianyu because it merges close-by edges to construct bounding boxes instead of the simple slicing method by horizontal/vertical lines. However, for GUIs with image background, its edge merging heuristics often fail due to the noisy edges of physical-world objects in the images. As such, it often reports some non-GUI-element regions of the image as element regions, or erroneously merges close-by elements, as shown in Figure 6. Furthermore, REMAUI merges text and non-text region heuristically, which are not very reliable either (see the text elements detected as non-text elements in REMAUI-(b)/(c)/(d)).

Deep learning models perform much better than old fashioned methods. In Figure 6, we see that they all locate some GUI elements accurately, even those overlaying on the background picture. These models are trained with large-scale data, "see" many sophisticated GUIs, and thus can locate GUI elements even in a noisy background. However, we also observe that the detected bounding boxes by deep learning models may not be very accurate, as they are estimated by a statistical regression model. The two-stage model Faster RCNN outperforms the other two one-stage models YOLOv3 and CenterNet. As discussed in Section 2.1, GUI elements have large in-class variance and high cross-class similarity. Two stage models perform region detection and region classification in a pipeline so that the region detection and region classification are less mutually interfered, compared with one-stage models that perform region detection and region classification simultaneously.

Between the two one-stage models, anchor-free CenterNet outperforms anchor-box-based YOLOv3 at IoU>0.9. However, YOLOv3 performs better than CenterNet at lower IoU thresholds (see Figure 3). Anchor-free model is flexible to handle the large in-class variance of GUI elements and GUI texts (see more experiments on GUI text detection in Section 3.5). However, as shown in Figure 6, this flexibility is a double-blade, which may lead to less accurate bounding boxes, or bound several elements in one box (e.g., CenterNet-(a)/(d)). Because GUI elements are often close-by or packed in a GUI, CenterNet very likely assembles the top-left and bottom-right corners of different GUI elements together, which leads to the wrong bounding boxes.

*Deep learning models significantly outperform old-fashioned detection methods. Two-stage anchor-box-based models perform the best in non-text GUI element detection task. But it is challenging for the deep learning models to achieve a good balance between the accuracy of the detected bounding boxes and the detected GUI elements, especially for anchor-free models.*

### 3.4 Results - RQ2 Sensitivity

This section reports the sensitivity analysis of the deep learning models for region detection from two aspects: anchor-box settings and amount of training data.

**3.4.1 Anchor-Box Settings.** For Faster RCNN, we use two settings: the default setting (three anchor-box scales - 128, 256 and 512, and three aspect ratios - 1:1, 1:2 and 2:1); and the customized setting (five anchor-box scales - 32, 64, 128, 256 and 512, and four aspect (width:height) ratios - 1:1, 2:1, 4:1 and 8:1). This customized setting is drawn from the frequent scales and aspect ratios of the GUI elements in our dataset. Considering the size of GUI elements, we add two small scales 32 and 64. Furthermore, we add two more aspect ratios to accommodate the large variance of GUI elements. For YOLOv3, we use two  $k$  settings: 5 and 9, which are commonly used in the literature. YOLOv3 automatically derives anchor-box metrics from  $k$  clusters of GUI images in the dataset. All models are trained using 40k training data and tested on 5k GUI images.

Table 3 shows the model performance (at IoU>0.9) of these different anchor-box settings. It is somehow surprising that there is only a small increase in F1 when we use more anchor-box scales and aspect ratios. We further compare the TPs of different anchor-box settings. We find that 55% of TPs overlap between the two settings for Faster RCNN, and 67% of TPs overlap between the two settings for YOLOv3. As the scales and aspect ratios of GUI elements follow standard distributions, using a smaller number of anchor boxes can still covers a large portion of the element distribution.

As different settings detect some different bounding boxes, we want to see if the differences may complement each other. To that end, we adopt two strategies to merge the detected boxes by the two settings: union strategy and intersection strategy. For two overlapped boxes, we take the maximum objectness of them, and then merge the two boxes by taking the union/intersection area for union/interaction strategy. For the rest of the boxes, we directly keep them. We find the best object confidence threshold for the combined results using the validation dataset. The union strategy does not significantly affect the F1, which means that making the bounding boxes larger is not very useful. In fact, for the boxes which are originally TPs by one setting, the enlarged box could even become FPs. However, the intersection strategy can boost the performance of both Faster RCNN and YOLOv3, achieving 0.456 and 0.427 in F1 respectively. It is reasonable because the intersection area is confirmed by the two settings, and thus more accurate.

**3.4.2 Amount of Training Data.** In this experiment, Faster RCNN uses the customized anchor-box setting and YOLOv3 uses  $k=9$ . We train the models with 2K, 10K, 40K training data separately, and test the models on the same 5k GUI images. Each 2k- or 10k experiment uses randomly selected 2k or 10k GUIs in the 40k training data. As shown in Table 4, the performance of all models drops as the

**Table 3: Impact of anchor-box settings (IoU>0.9)**

Setting	Precision	Recall	F1
Faster RCNN Default	0.433	0.410	0.421
Faster RCNN Customized	0.440	0.437	0.438
Faster RCNN Union	0.394	0.469	0.428
Faster RCNN Intersection	<b>0.452</b>	<b>0.460</b>	<b>0.456</b>
YOLOv3 k=5	0.394	0.333	0.361
YOLOv3 k=9	0.405	0.363	0.383
YOLO Union	0.372	0.375	0.373
YOLO Intersection	<b>0.430</b>	<b>0.424</b>	<b>0.427</b>

**Table 4: Impact of amount of training data (IoU>0.9)**

Method	Size	Precision	Recall	F1
Faster-RCNN	2K	0.361	0.305	0.331
	10K	0.403	0.393	0.398
	40K	<b>0.440</b>	<b>0.437</b>	<b>0.438</b>
YOLOv3	2K	0.303	0.235	0.265
	10K	0.337	0.293	0.313
	40K	<b>0.405</b>	<b>0.363</b>	<b>0.383</b>
CenterNet	2K	0.319	0.313	0.316
	10K	0.328	0.329	0.329
	40K	<b>0.424</b>	<b>0.380</b>	<b>0.401</b>

**Table 5: Text detection: separated versus unified processing**

Method	Element	Precision	Recall	F1
Faster-RCNN	nontext-only	0.440	0.437	0.438
	nontext	<b>0.379</b>	<b>0.436</b>	<b>0.405</b>
	mix	0.275	0.250	0.262
	text	0.351	0.359	0.355
YOLOv3	nontext-only	0.405	0.363	0.383
	non-text	0.325	0.347	0.335
	mix	0.319	0.263	0.288
	text	0.355	0.332	0.343
CenterNet	nontext-only	0.424	0.380	0.401
	non-text	0.321	0.397	0.355
	mix	<b>0.416</b>	<b>0.319</b>	<b>0.361</b>
	text	<b>0.391</b>	<b>0.385</b>	<b>0.388</b>

training data decreases. This is reasonable because deep learning models cannot effectively learn the essential features of the GUI elements without sufficient training data. The relative performance of the three models is consistent at the three training data sizes, with YOLOv3 always being the worst. This indicates the difficulty in training one-stage anchor-box model. Faster RCNN with 2k (or 10k) training data achieves the comparable or higher F1 than that of YOLOv3 and CenterNet with 10k (or 40k) training data. This result further confirms that two-stage model fits better for GUI element detection tasks than one-stage model, and one-stage anchor-free model performs better than one-stage anchor-box model.

*Anchored settings do not significantly affect the performance of anchored-based models, because a small number of anchor boxes can cover the majority of GUI elements. Two-stage anchored-based model is the easiest to train, which requires one magnitude less training data to achieve comparable performance as one-stage model. One stage anchored model is the most difficult to train.*

**Table 6: Text detection: OCR versus scene text**

Method	Precision	Recall	F1
Tesseract	0.291	0.518	0.372
EAST	<b>0.402</b>	<b>0.720</b>	<b>0.516</b>
REMAUI	0.297	0.505	0.374
Xianyu	0.271	0.486	0.348

### 3.5 Results - RQ3 Text Detection

*3.5.1 Separated versus Unified Text/Non-Text Element Detection.* All existing works detect GUI text separately from non-text elements. This is intuitive in that GUI text and non-text elements have very different visual features. However, we were wondering if this is a must or text and non-text elements can be reliably detected by a single model. To answer this, we train Faster RCNN, YOLOv3 and CenterNet to detect both text and non-text GUI elements. Faster RCNN uses the customized anchor-box setting and YOLOv3 uses  $k=9$ . The model is trained with 40k data and tested on 5k GUI images. In this RQ, both non-text and text elements in GUIs are used for model training and testing.

Table 5 shows the results. When trained to detect text and non-text elements together, Faster RCNN still performs the best in terms of detecting non-text elements. But the performance of all three models for detecting non-text elements degrades, compared with the models trained to detect non-text elements only. This indicates that mixing the learning of text and non-text element detection together interfere with the learning of detecting non-text elements. CenterNet performs much better for detecting text elements than Faster RCNN and YOLOv3, which results in the best overall performance for the mixed text and non-text detection. CenterNet is anchor-free, which makes it flexible to handle large variance of text patterns. So it has comparable performance for text and non-text elements. In contrast, anchor-box-based Faster RCNN and YOLOv3 are too rigid to reliably detect text elements. However, the performance of CenterNet in detecting text elements is still poor. Text elements always have space between words and lines. Due to the presence of these spaces, CenterNet often detects a partial text element or erroneously groups separate text elements as one element when assembling object corners.

*3.5.2 OCR versus Scene Text Recognition.* Since it is not feasible to detect text and non-text GUI elements within a single model, we want to investigate what is the most appropriate method for GUI text detection. All existing works (e.g., REMAUI, Xianyu) simply use OCR tool like Tesseract. We observe that GUI text is more similar to scene text than to document text. Therefore, we adopt a deep learning scene text recognition model EAST for GUI text detection, and compare it with Tesseract. We directly use the pre-trained EAST model without any fine tuning on GUI text.

As shown in Table 6, EAST achieves 0.402 in precision, 0.720 in recall and 0.516 in F1, which is significantly higher than Tesseract (0.291 in precision, 0.518 in recall and 0.372 in F1). Both Xianyu and REMAUI perform some post-processing of the Tesseract's OCR results in order to filter out false positives. But it does not significantly change the performance of GUI text detection. As EAST is specifically designed for scene text recognition, its performance is significantly better than using generic object detection models for GUI text detection (see Table 5). EAST detects almost all texts in

a GUI, including those on the GUI widgets (e.g., the button labels in Figure 4(c)). However, those texts on GUI widgets are considered as part of the widgets in our ground-truth data, rather than stand-alone texts. This affects the precision of EAST against our ground-truth data, even though the detected texts are accurate.

Figure 4 presents some detection results. Tesseract achieves the comparable results as EAST only for the left side of Figure 4(d), where text is shown on a white background just like in a document. From all other detection results, we can observe the clear advantages of treating GUI text as scene text than as document text. First, EAST can accurately detect text in background image (Figure 4(a)), while Tesseract outputs many inaccurate boxes in such images. Second, EAST can detect text in a low contrast background (Figure 4(b)), while Tesseract often misses such texts. Third, EAST can ignore non-text elements (e.g., the bottom-right switch buttons in Figure 4(b), and the icons on the left side of Figure 4(d)), while Tesseract often erroneously detects such non-text elements as text elements.

*GUI text and non-text elements should be detected separately. Neither OCR techniques nor generic object detection models can reliably detect GUI texts. As GUI texts have the characteristics of scene text, the deep learning scene text recognition model can be used (even without fine-tuning) to accurately detect GUI texts.*

## 4 A NOVEL APPROACH

Based on the findings in our empirical study, we design a novel approach for GUI element detection. Our approach combines the simplicity of old-fashioned computer vision methods for non-text-element region detection, and the mature, easy-to-deploy deep learning models for region classification and GUI text detection (Section 4.1). This synergy achieves the state-of-the-art performance for the GUI element detection task (Section 4.2).

### 4.1 Approach Design

Our approach detects non-text GUI elements and GUI texts separately. For GUI text detection, we simply use the pre-trained state-of-the-art scene text detector EAST [49]. For non-text GUI element detection, we adopt the two-stage design, i.e., perform region detection and region classification in a pipeline. For region detection, we develop a novel old-fashioned method with a top-down coarse-to-fine strategy and a set of GUI-specific image processing algorithms. For region classification, we fine-tune the pre-trained ResNet50 image classifier [20] with GUI element images.

**4.1.1 Region Detection for Non-Text GUI Elements.** According to the performance and sensitivity experiments results, we do not want to use generic deep learning object detection models [13, 32, 35]. First, they demand sufficient training data, and different model designs require different scale of training data to achieve stable performance. Furthermore, the model performance is still less optimal even with a large set of training data, and varies across different model designs. Second, the nature of statistical regression based region detection cannot satisfy the high accuracy requirement of GUI element detection. Unlike generic object detection where a typical correct detection is defined loosely (e.g., IoU>0.5) [14], detecting GUI elements is a fine-grained recognition task which requires a correct detection that covers the full region of the GUI



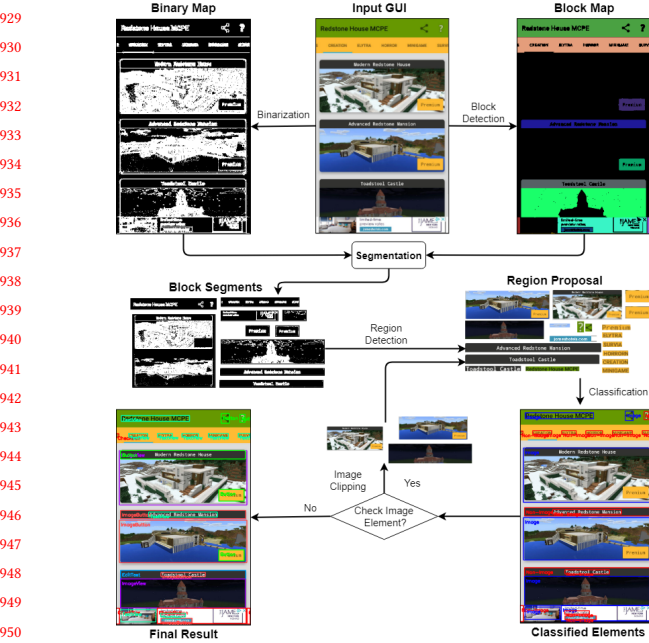
Figure 4: Examples: OCR versus scene text

elements as accurate as possible, but the region of non-GUI elements and other close-by GUI elements as little as possible. Unfortunately, neither anchor-box based nor anchor-free models can achieve this objective, because they are either too strict or too flexible in face of large in-class variance of element sizes and texture, high cross-class shape similarity, and the presence of close-by GUI elements.

Unlike deep learning models, old-fashioned methods [28, 46] do not require any training which makes them easy to deploy. Furthermore, when old fashioned methods locate some GUI elements, the detected bounding boxes are usually accurate, which is desirable. Therefore, we adopt old-fashioned methods for non-text GUI-element region detection. However, existing old-fashioned methods use a bottom-up strategy which aggregates the fine details of the objects (e.g., edge or contour) into objects. This bottom-up strategy performs poorly, especially affected by the complex background or objects in the GUIs and GUI elements. As shown in Figure 5, our method adopts a completely different strategy: top-down coarse-to-fine. This design carefully considers the regularity of GUI layouts and GUI-element shapes and boundaries, as well as the significant differences between the shapes and boundaries of artificial GUI elements and those of physical-world objects.

Our region detection method first detects the layout blocks of a GUI. The intuition is that GUIs organize GUI elements into distinct blocks, and these blocks generally have rectangle shape. Xianyu also detects blocks, but it assumes the presence of clear horizontal and vertical lines. Our method does not make this naive assumption. Instead, it first uses the flood-filling algorithm [42] over the grey-scale map of the input GUI to obtain the maximum regions with similar colors, and then uses the shape recognition [31] to determine if a region is a rectangle. Each rectangle region is considered as a block. Finally, it uses the Sklansky's algorithm [39] to compute the boundary of the block and produce a block map. In Figure 5, we show the detected block in different colors for the presentation clarity. Note that blocks usually contain some GUI elements, but some blocks may correspond to a particular GUI element.

Next, our method generates a binary map of the input GUI, and for each detected block, it segments the corresponding region of the binary map. Binarization simplifies the input image into a black-white image, on which the foreground GUI elements can be

**Figure 5: Our method for non-text GUI element detection**

separated from the background. Existing methods [28, 46] perform binarization through Canny edge detection [7] and Sobel edge detection [16], which are designed to keep fine texture details in nature scene images. Unfortunately, this detail-keeping capability contradicts the goal of GUI element detection, which is to detect the shape of GUI elements, rather than their content and texture details. For example, we want to detect an ImageView element no matter what objects are shown in the image (see Figure 6). We develop a simple but effective binarization method based on the gradient map [17] of the GUI images. A gradient map captures the change of gradient magnitude between neighboring pixels. If a pixel has small gradient with neighboring pixels, it becomes black on the binary map, otherwise white. As shown in Figure 5, the GUI elements stand out from the background in the binary map, either as white region on the black background or black region with white edge.

Our method uses the connected component labeling [36] to identify GUI element regions in each binary block segment. As GUI elements can be any shape, it identifies a smallest rectangle box that covers the detected regions as the bounding boxes. Although our binarization method does not keep many texture details of non-GUI objects, the shape of non-GUI objects (e.g., those buildings in the pictures) may still be present in the binary map. These noisy shapes interfere existing bottom-up aggregation methods [7, 39] for GUI element detection, which results in over-segmentation of GUI elements. In contrast, our top-down detection strategy minimizes the influence of these non-GUI objects, because it uses relaxed grey-scale map to detect large blocks and then uses strict binary map to detect GUI elements. If a block is classified as an image, our method will not further detect GUI elements in this block.

**4.1.2 Region Classification for Non-Text GUI Elements.** For each detected GUI element region in the input GUI, we use a ResNet50 image classifier to predict its element type. In this work, we consider 15 element types as shown in Figure 1. The Resnet50 image classifier

**Table 7: Detection performance of our approach (IoU>0.9)**

Elements	Precision	Recall	F1
non-text	0.503	0.545	0.523
text	0.589	0.547	0.516
both	0.539	0.612	0.573

**Table 8: Region classification results for TP regions**

Method	Non-text elements			All elements		
	#bbox	Accuracy	#bbox	Accuracy	#bbox	Accuracy
FasterRCNN	18,577	0.68	34,915	0.68		
YOLOv3	15,428	0.64	32,225	0.65		
Centernet	16,072	0.68	36,803	0.66		
Our method	21,977	<b>0.86</b>	53,027	<b>0.91</b>		

**Table 9: Overall results of object detection (IoU > 0.9)**

Method	Non-text elements			All elements		
	Precision	Recall	F1	Precision	Recall	F1
Faster-RCNN	0.316	0.313	0.315	0.269	0.274	0.271
YOLOv3	0.274	0.246	0.260	0.258	0.242	0.249
CenterNet	0.302	0.270	0.285	0.284	0.280	0.282
Our method	<b>0.431</b>	<b>0.469</b>	<b>0.449</b>	<b>0.490</b>	<b>0.557</b>	<b>0.524</b>

is pre-trained with the ImageNet data. We fine-tune the pre-trained model with 90,000 GUI elements (6,000 per element type) randomly selected from the 40k GUIs in our training dataset.

**4.1.3 GUI Text Detection.** Section 3.5 shows that GUI text should be treated as scene text and be processed separately from non-text elements. Furthermore, scene text recognition model performs much better than generic object detection models. Therefore, we use the state-of-the-art deep-learning scene text detector EAST [49] to detect GUI text. As shown in Figure 4(c), EAST may detect texts that are part of non-image GUI widgets (e.g., the text on the buttons). Therefore, if the detected GUI text is inside the region of a non-image GUI widgets, we discard this text.

## 4.2 Evaluation

We evaluate our approach on the same testing data used in our empirical study by 5-fold cross-validation. Table 7 shows the region-detection performance for non-text, text and both types of elements. For non-text GUI elements, our approach performs better than the best baseline Faster RCNN (0.523 versus 0.438 in F1). For text elements, our approach is overall the same as EAST. It is better than EAST in precision, because our approach discards some detected texts that are a part of GUI widgets. But this degrades the recall. For text and non-text elements as a whole, our approach performs better than the best baseline CenterNet (0.573 versus 0.388 in F1).

Figure 6 shows the examples of the detection results by our approach and the five baselines. Compared with REMAUI and Xianyu, our method detects much more GUI elements and much less noisy non-GUI element regions, because of our robust top-down coarse-to-fine strategy and GUI-specific image processing (e.g., connected component labeling rather than canny edge and contour). Our method also detects more GUI elements than the three deep learning models. Furthermore, it outputs more accurate bounding boxes and less overlapping bounding boxes, because our method performs accurate pixel analysis rather than statistical regression in the high-layer of CNN. Note that deep learning models may detect objects in images as GUI elements, because there are GUI elements of that size and with similar visual features. In contrast, our method detects



Figure 6: Region detection results for non-text GUI element: our method versus five baselines

large blocks that are images and treats such images as whole. As such, our method suffers less over-segmentation problem.

Table 8 shows the region classification results of our CNN classifier and the three deep learning baselines. The results consider only true-positive bounding boxes, i.e., the classification performance given the accurate element regions. As text elements are outputted by EAST directly, we show the results for non-text elements and all elements. We can see that our method outputs more true-positive GUI element regions, and achieves higher classification accuracy (0.86 for non-text elements and 0.91 for all elements, and the other three deep models achieves about 0.68 accuracy). Our classification accuracy is consistent with [26], which confirms that the effectiveness of a pipeline design for GUI element detection.

Table 9 shows the overall object detection results, i.e., the true-positive bounding box with the correct region classification over all detected element regions. Among the three baseline models, Faster RCNN performs the best for non-text elements (0.315 in F1), but CenterNet, due to this model flexibility to handle GUI texts, achieves the best performance for all elements (0.282 in F1). Compared with these three baselines, our method achieves much better F1 for both non-text elements (0.449) and all elements (0.524), due to its strong capability in both region detection and region classification.

## 5 RELATED WORK

GUI design, implementation and testing are important software engineering tasks, to name a few, GUI code generation [5, 9, 26], GUI search [8, 21, 48], GUI design examination [27, 41, 47], reverse-engineering GUI dataset [11], GUI accessibility [10], and GUI testing [4, 22, 30, 43]. Many of these tasks require the detection of GUI elements. Table 1 and Section 3.2.2 summarizes the old-fashioned

methods (e.g., REMAUI [28] and Xianyu [46]) designed for GUI element detection, the generic object detection models (Faster RCNN, YOLOv3 and CenterNet) applied for non-text GUI element detection, and the old-fashioned OCR tool Tesseract [37] and the state-of-the-art scene text detector EAST [49] for GUI text detection. Readers are referred to previous sections for details. Our empirical study shows that old-fashioned methods perform poorly for both text and non-text GUI element detection. Generic object detection models perform better than old-fashioned ones, but they cannot satisfy the high accuracy requirement of GUI element detection. Our method advances the state-of-the-art in GUI element detection by effectively assembling the effective designs of existing methods and a novel GUI-specific old-fashioned region detection method.

## 6 CONCLUSION

This paper investigates the problem of GUI element detection. We identify four unique characteristics of GUIs and GUI elements, including large in-class variance, high cross-class similarity, packed or close-by elements and mix of heterogeneous objects. These characteristics make it a challenging task for existing methods (no matter old fashioned or deep learning) to accurately detect GUI elements in GUI images. Our empirical study reveals the underperformance of existing methods borrowed from computer vision domain and the underlying reasons, and identifies the effective designs of GUI element detection methods. Informed by our study findings, we design a new GUI element detection approach with both the effective designs of existing methods and the GUI characteristics in mind. Our new method achieves the state-of-the-art performance on the largest-ever evaluation of GUI element detection methods.

1045  
1046  
1047  
1048  
1049  
1050  
1051  
1052  
1053  
1054  
1055  
1056  
1057  
1058  
1059  
1060  
1061  
1062  
1063  
1064  
1065  
1066  
1067  
1068  
1069  
1070  
1071  
1072  
1073  
1074  
1075  
1076  
1077  
1078  
1079  
1080  
1081  
1082  
1083  
1084  
1085  
1086  
1087  
1088  
1089  
1090  
1091  
1092  
1093  
1094  
1095  
1096  
1097  
1098  
1099  
1100  
1101  
1102  
1103  
1104  
1105  
1106  
1107  
1108  
1109  
1110  
1111  
1112  
1113  
1114  
1115  
1116  
1117  
1118  
1119  
1120  
1121  
1122  
1123  
1124  
1125  
1126  
1127  
1128  
1129  
1130  
1131  
1132  
1133  
1134  
1135  
1136  
1137  
1138  
1139  
1140  
1141  
1142  
1143  
1144  
1145  
1146  
1147  
1148  
1149  
1150  
1151  
1152  
1153  
1154  
1155  
1156  
1157  
1158  
1159  
1160

## REFERENCES

- [1] Nikola Banovic, Tovi Grossman, Justin Matejka, and George Fitzmaurice. 2012. Waken: reverse engineering usage information and interface structure from software videos. In *Proceedings of the 25th annual ACM symposium on User interface software and technology*. 83–92.
- [2] Lingfeng Bao, Jing Li, Zhenchang Xing, Xinyu Wang, and Bo Zhou. 2015. scvRipper: video scraping tool for modeling developers' behavior using interaction data. In *2015 IEEE/ACM 37th IEEE International Conference on Software Engineering*, Vol. 2. IEEE, 673–676.
- [3] Lingfeng Bao, Deheng Ye, Zhenchang Xing, Xin Xia, and Xinyu Wang. 2015. Activityspace: a remembrance framework to support interapplication information needs. In *2015 30th IEEE/ACM International Conference on Automated Software Engineering (ASE)*. IEEE, 864–869.
- [4] Carlos Bernal-Cárdenas, Nathan Cooper, Kevin Moran, Oscar Chaparro, Andrian Marcus, and Denys Poshyvanyk. 2020. Translating Video Recordings of Mobile App Usages into Replayable Scenarios. In *42nd International Conference on Software Engineering (ICSE '20)*. ACM, New York, NY.
- [5] Pavol Bielik, Marc Fischer, and Martin Vechev. 2018. Robust relational layout synthesis from examples for Android. *Proceedings of the ACM on Programming Languages* 2, OOPSLA (2018), 1–29.
- [6] Karl Bridge and Michael Satran. 2018. *Windows Accessibility API overview*. Retrieved March 2, 2020 from <https://docs.microsoft.com/en-us/windows/win32/winauto/windows-automation-api-portal>
- [7] J. Canny. 1986. A Computational Approach to Edge Detection. *IEEE Transactions on Pattern Analysis and Machine Intelligence PAMI-8*, 6 (Nov 1986), 679–698. <https://doi.org/10.1109/TPAMI.1986.4767851>
- [8] Chunyang Chen, Sidong Feng, Zhenchang Xing, Linda Liu, Shengdong Zhao, and Jinshui Wang. 2019. Gallery DC: Design Search and Knowledge Discovery through Auto-created GUI Component Gallery. *Proceedings of the ACM on Human-Computer Interaction* 3, CSCW (2019), 1–22.
- [9] Chunyang Chen, Ting Su, Guozhu Meng, Zhenchang Xing, and Yang Liu. 2018. From UI design image to GUI skeleton: a neural machine translator to bootstrap mobile GUI implementation. In *Proceedings of the 40th International Conference on Software Engineering*. 665–676.
- [10] Jieshan Chen, Chunyang Chen, Zhenchang Xing, Xiwei Xu, Liming Zhu, Guoqiang Li, and Jinshui Wang. 2020. Unblind Your Apps: Predicting Natural-Language Labels for Mobile GUI Components by Deep Learning. In *42nd International Conference on Software Engineering (ICSE '20)*. ACM, New York, NY, 13 pages. <https://doi.org/10.1145/3377811.3380327>
- [11] Biplob Deka, Zifeng Huang, Chad Franzen, Joshua Hibscher, Daniel Afergan, Yang Li, Jeffrey Nichols, and Ranjitha Kumar. 2017. Rico: A mobile app dataset for building data-driven design applications. In *Proceedings of the 30th Annual ACM Symposium on User Interface Software and Technology*. 845–854.
- [12] Morgan Dixon and James Fogarty. 2010. Prefab: implementing advanced behaviors using pixel-based reverse engineering of interface structure. In *Proceedings of the SIGCHI Conference on Human Factors in Computing Systems*. 1525–1534.
- [13] Kaiwen Duan, Song Bai, Lingxi Xie, Honggang Qi, Qingming Huang, and Qi Tian. 2019. Centernet: Keypoint triplets for object detection. In *Proceedings of the IEEE International Conference on Computer Vision*. 6569–6578.
- [14] Mark Everingham, Luc Van Gool, Christopher K. I. Williams, John Winn, and Andrew Zisserman. 2009. The Pascal Visual Object Classes (VOC) Challenge. *International Journal of Computer Vision* 88, 2 (Sep 2009), 303–338. <https://doi.org/10.1007/s11263-009-0275-4>
- [15] Mark Everingham, Luc Van Gool, Christopher KI Williams, John Winn, and Andrew Zisserman. 2010. The pascal visual object classes (voc) challenge. *International journal of computer vision* 88, 2 (2010), 303–338.
- [16] Rafael C. Gonzalez and Richard E. Woods. 1993. *Digital image processing*. Addison-Wesley.
- [17] Rafael C. Gonzalez and Richard E. Woods. 2014. *Digital image processing*. Dorling Kindersley.
- [18] Google. 2019. *UI Automator*. Retrieved March 2, 2020 from <https://developer.android.com/training/testing/ui-automator>
- [19] Google. 2020. *Build more accessible apps*. Retrieved March 2, 2020 from <https://developer.android.com/guide/topics/ui/accessibility>
- [20] Kaiming He, Xiangyu Zhang, Shaoqing Ren, and Jian Sun. 2016. Deep residual learning for image recognition. In *Proceedings of the IEEE conference on computer vision and pattern recognition*. 770–778.
- [21] Forrest Huang, John F Canny, and Jeffrey Nichols. 2019. Swire: Sketch-based user interface retrieval. In *Proceedings of the 2019 CHI Conference on Human Factors in Computing Systems*. 1–10.
- [22] Yuanchun Li, Ziyue Yang, Yao Guo, and Xiangqun Chen. 2019. Humanoid: A Deep Learning-Based Approach to Automated Black-box Android App Testing. In *2019 34th IEEE/ACM International Conference on Automated Software Engineering (ASE)*. IEEE, 1070–1073.
- [23] Feng Lin, Chen Song, Xiaowei Xu, Lora Cavuoto, and Wenya Xu. 2016. Sensing from the bottom: Smart insole enabled patient handling activity recognition through manifold learning. In *2016 IEEE First International Conference on Connected Health: Applications, Systems and Engineering Technologies (CHASE)*. IEEE, 254–263.
- [24] Tsung-Yi Lin, Michael Maire, Serge Belongie, James Hays, Pietro Perona, Deva Ramanan, Piotr Dollár, and C Lawrence Zitnick. 2014. Microsoft coco: Common objects in context. In *European conference on computer vision*. Springer, 740–755.
- [25] Microsoft. 2016. *Introducing Spy++*. Retrieved March 2, 2020 from <https://docs.microsoft.com/en-us/visualstudio/debugger/introducing-spy-increment?view=vs-2019>
- [26] Kevin Moran, Carlos Bernal-Cárdenas, Michael Curcio, Richard Bonett, and Denys Poshyvanyk. 2018. Machine learning-based prototyping of graphical user interfaces for mobile apps. *arXiv preprint arXiv:1802.02312* (2018).
- [27] Kevin Moran, Boyang Li, Carlos Bernal-Cárdenas, Dan Jelf, and Denys Poshyvanyk. 2018. Automated reporting of GUI design violations for mobile apps. In *Proceedings of the 40th International Conference on Software Engineering*. 165–175.
- [28] Tuan Anh Nguyen and Christoph Csallner. 2015. Reverse engineering mobile application user interfaces with remau (t). In *2015 30th IEEE/ACM International Conference on Automated Software Engineering (ASE)*. IEEE, 248–259.
- [29] Suporn Pongnumkul, Mira Dontcheva, Wilmot Li, Jue Wang, Lubomir Bourdev, Shai Avidan, and Michael F Cohen. 2011. Pause-and-play: automatically linking screencast video tutorials with applications. In *Proceedings of the 24th annual ACM symposium on User interface software and technology*. 135–144.
- [30] Ju Qian, Zhengyu Shang, Shuoyan Yan, Yan Wang, and Lin Chen. 2020. RoScript: A Visual Script Driven Truly Non-Intrusive Robotic Testing System for Touch Screen Applications. In *42nd International Conference on Software Engineering (ICSE '20)*. ACM, New York, NY.
- [31] Urs Ramer. 1972. An iterative procedure for the polygonal approximation of plane curves. *Computer Graphics and Image Processing* 1, 3 (1972), 244–256. [https://doi.org/10.1016/s0146-664x\(72\)80017-0](https://doi.org/10.1016/s0146-664x(72)80017-0)
- [32] Joseph Redmon and Ali Farhadi. 2017. YOLO9000: better, faster, stronger. In *Proceedings of the IEEE conference on computer vision and pattern recognition*. 7263–7271.
- [33] Joseph Redmon and Ali Farhadi. 2018. Yolov3: An incremental improvement. *arXiv preprint arXiv:1804.02767* (2018).
- [34] Steven P Reiss, Yun Miao, and Qi Xin. 2018. Seeking the user interface. *Automated Software Engineering* 25, 1 (2018), 157–193.
- [35] Shaqoing Ren, Kaiming He, Ross Girshick, and Jian Sun. 2015. Faster r-cnn: Towards real-time object detection with region proposal networks. In *Advances in neural information processing systems*. 91–99.
- [36] H. Samet and M. Tamminen. 1988. Efficient component labeling of images of arbitrary dimension represented by linear bintrees. *IEEE Transactions on Pattern Analysis and Machine Intelligence* 10, 4 (1988), 579–586. <https://doi.org/10.1109/34.3918>
- [37] Ray Smith. 2007. An overview of the Tesseract OCR engine. In *Ninth International Conference on Document Analysis and Recognition (ICDAR 2007)*, Vol. 2. IEEE, 629–633.
- [38] Mohian Soumik. 2019. *pix2app*. Retrieved March 2, 2020 from <https://github.com/soumikmohian/pix2app>
- [39] Satoshi Suzuki and Keiichi A be. 1985. Topological structural analysis of digitized binary images by border following. *Computer Vision, Graphics, and Image Processing* 30, 1 (1985), 32 – 46. [https://doi.org/10.1016/0734-189X\(85\)90016-7](https://doi.org/10.1016/0734-189X(85)90016-7)
- [40] Amanda Sweeney, Mira Dontcheva, Wilmot Li, Joel Brandt, Morgan Dixon, and Andrew J Ko. 2018. Rewrite: Interface design assistance from examples. In *Proceedings of the 2018 CHI Conference on Human Factors in Computing Systems*. 1–12.
- [41] Amanda Sweeney and Yang Li. 2019. Modeling Mobile Interface Tappability Using Crowdsourcing and Deep Learning. In *Proceedings of the 2019 CHI Conference on Human Factors in Computing Systems*. 1–11.
- [42] Shane Torbert. 2016. *Applied computer science*. Springer.
- [43] Thomas D White, Gordon Fraser, and Guy J Brown. 2019. Improving random GUI testing with image-based widget detection. In *Proceedings of the 28th ACM SIGSOFT International Symposium on Software Testing and Analysis*. 307–317.
- [44] Jing Yang, Qingshan Liu, and Kaihua Zhang. 2017. Stacked hourglass network for robust facial landmark localisation. In *Proceedings of the IEEE Conference on Computer Vision and Pattern Recognition Workshops*. 79–87.
- [45] Tom Yeh, Tsung-Hsiang Chang, and Robert C Miller. 2009. Sikuli: using GUI screenshots for search and automation. In *Proceedings of the 22nd annual ACM symposium on User interface software and technology*. 183–192.
- [46] Chen Yongxin, Zhang Tonghui, and Chen Jie. 2019. *UI2code: How to Fine-tune Background and Foreground Analysis*. Retrieved Feb 23, 2020 from <https://laptrinhx.com/ui2code-how-to-fine-tune-background-and-foreground-analysis-2293652041/>
- [47] Dehai Zhao, Zhenchang Xing, Chunyang Chen, Xiwei Xu, Liming Zhu, Guoqiang Li, and Jinshui Wang. 2020. Seenomaly: Vision-Based Linting of GUI Animation Effects Against Design-Donâ€¢t Guidelines. In *42nd International Conference on Software Engineering (ICSE '20)*. ACM, New York, NY, 12 pages. <https://doi.org/10.1145/3377811.3380411>

- 1277 [48] Shuyu Zheng, Ziniu Hu, and Yun Ma. 2019. FaceOff: Assisting the Manifestation  
1278 Design of Web Graphical User Interface. In *Proceedings of the Twelfth ACM*  
1279 *International Conference on Web Search and Data Mining*. 774–777.
- 1280
- 1281
- 1282
- 1283
- 1284
- 1285
- 1286
- 1287
- 1288
- 1289
- 1290
- 1291
- 1292
- 1293
- 1294
- 1295
- 1296
- 1297
- 1298
- 1299
- 1300
- 1301
- 1302
- 1303
- 1304
- 1305
- 1306
- 1307
- 1308
- 1309
- 1310
- 1311
- 1312
- 1313
- 1314
- 1315
- 1316
- 1317
- 1318
- 1319
- 1320
- 1321
- 1322
- 1323
- 1324
- 1325
- 1326
- 1327
- 1328
- 1329
- 1330
- 1331
- 1332
- 1333
- 1334
- 1335 [49] Xinyu Zhou, Cong Yao, He Wen, Yuzhi Wang, Shuchang Zhou, Weiran He,  
1336 and Jiajun Liang. 2017. EAST: an efficient and accurate scene text detector. In  
1337 *Proceedings of the IEEE conference on Computer Vision and Pattern Recognition*.  
1338 5551–5560.
- 1339
- 1340
- 1341
- 1342
- 1343
- 1344
- 1345
- 1346
- 1347
- 1348
- 1349
- 1350
- 1351
- 1352
- 1353
- 1354
- 1355
- 1356
- 1357
- 1358
- 1359
- 1360
- 1361
- 1362
- 1363
- 1364
- 1365
- 1366
- 1367
- 1368
- 1369
- 1370
- 1371
- 1372
- 1373
- 1374
- 1375
- 1376
- 1377
- 1378
- 1379
- 1380
- 1381
- 1382
- 1383
- 1384
- 1385
- 1386
- 1387
- 1388
- 1389
- 1390
- 1391
- 1392